Indoor Carrier Phase Tracking and Positioning with Difference Correlators

T. Pany[(1)], H.-J. Euler[(2)] and J. Winkel[(1)]

[(1)]*IFEN GmbH, Alte Gruber Straße 6, 85586 Poing, Germany,*

[(2)]*inPosition gmbh, PO Box 313, 9435 Heerbrugg, Switzerland*

BIOGRAPHIES

Dr. Thomas Pany works for IFEN GmbH as a senior research engineer in the GNSS receiver department. In particular, he is concerned with algorithm development and C/C++/assembler coding. He also works as a lecturer (Priv.-Doz.) at the University FAF Munich. His research interests include GNSS receivers, GNSS/INS integration, signal processing and GNSS science.

Dr. Hans-Jürgen Euler studied at the Technical University of Darmstadt. He has been awarded his PhD degree for fast integer ambiguity resolution for dual frequency GPS. After working for Terrasat (now Trimble) and Leica Geosystems he founded inPosition gmbh in 2006. InPosition does algorithm and concept development in the area of precise GNSS positioning.

Dr. Jón Ó. Winkel is head of receiver technology at IFEN GmbH since 2001. He studied physics at the universities in Hamburg and Regensburg. He received a PhD (Dr.-Ing.) from the University of the FAF in Munich in 2003 on GNSS modeling and simulations.

ABSTRACT

Single and double difference (code and carrier) observations are well known concepts in precise positioning to eliminate common mode errors. Difference correlators extend this concept to the level of correlator values. By doing that, the same common mode errors (e.g. clock errors) are cancelled thereby drastically reducing the signal dynamics. Then much smaller loop bandwidths or longer integration times can be applied to reduce noise and to eliminate multipath contributions. For static applications a coherent integration time of 100 s gives a single channel carrier tracking sensitivity of -14 dBHz (!), provided that code and Doppler lock can be achieved by e.g. vector tracking. Indoor carrier phase tracking is possible. Phase delays caused by the penetration of building materials determine the accuracy limit. A method is proposed to identify time windows with approximately constant delays. L1CA and L2CM indoor data show periods of e.g. 16 min, where propagation delays remain within a few centimeters variation and it is possible to compute an indoor position using carrier phases only (no code pseudoranges) with an accuracy of 1 m.

INTRODUCTION

The difference correlator processing is performed with two GNSS software receivers (SX-NSR), one acting as a rover, and the other acting as reference station. The data evaluation is currently done in post-processing but can in principle be done also in real-time. The reference station retrieves navigation data bits of the tracked satellite signals and stores them into a file. Furthermore, the reference station generates a RINEX observation file. The rover collects IF samples and stores them onto a hard disc. All data from the reference station and the rover are input to the post-processing, which produces a new (improved) RINEX observation file for the rover. A GPS data processing software then analyzes the reference and rover RINEX files to estimate the rover position.

Loosely speaking, the prompt correlator of a GNSS tracking channel is the exponential of the estimated carrier phase. Thus a (receiver) single difference correlator is obtained by multiplying the rover prompt correlator with the exponential of the corresponding reference station carrier phase and the broadcast navigation data bit. This principle can be extended to double (receiver and satellite) differences and will be precisely described in the paper. The signal dynamics in a double difference correlator can be very low. For example, for a static user and baseline length of 50 m, the remaining acceleration is around 50 $\mu m/s^2$. Thus we can form coherent batches of several hundreds of seconds (in our test we used a maximum of 30 s) and use those batches to estimate the double difference carrier phase.

Ideally the double difference correlators within one batch represent a tone signal, and the frequency is the (double difference) Doppler frequency. The phase of the tone signal relates to the user position. An adaptive filter detects the dominant frequency contribution of the line-of-sight signal and applies a linear filter. Ideally, only the

line-of-sight signal passes through and multipath signals (having a slightly different Doppler) and noise can be filtered out. The frequency selectivity is inversely proportional to the batch length (e.g. 33 mHz). The separation of those components is completely carried out in frequency domain, whereas a conventional PLL smoothes carrier phase estimates in the time domain. Finally, an estimator derives the Doppler frequency and the carrier phase at a given reference epoch from the filtered signal to write them into a RINEX file. This process includes unwrapping and undoing the differencing process with certain assumptions on the receiver clock.

A typical standard PLL works with a tracking loop bandwidth of 5-15 Hz, even if the receiver is operated in a static mode, to cope with user oscillator variations. On contrast, a batch length of 100 s corresponds to a equivalent loop bandwidth 0.05 Hz. Provided that the tracking channel can maintain code and Doppler lock (e.g via aiding from other channels = vector tracking), then we can show theoretically that a carrier tracking sensitivity of -14 dBHz is possible.

Our indoor test (with a batch length of 30 s) verify this high tracking sensitivity. A network of precisely surveyed indoor reference points was established in the IFEN office. With the rover antenna on one of the reference points located in a conference room of IFEN, we can track continuously the carrier phase of all satellites on L1C/A and L2CM. The phase and Doppler estimates based on the individual batches are highly consistent in the sense that phase difference between two batches well relates to the estimated Doppler. Estimates from timely adjacent batches are uncorrelated. It is well known that indoor signals have strong multipath and fading effects. With the difference correlator and using data from L1 and L2 of the same channel, we can verify them.

Especially the presence of the biases are certainly introducing challenges for position determinations based on the observation data tracked indoors. The differential position between an open-sky reference station and the indoor rover provided an impressive sub-meter accuracy. Those result certainly trigger the next question of how to utilize the carriers for possible indoor positioning cases. The paper presents some preliminary indoor positions based on carrier phases.

CONCEPT

Single and double difference observations (code and carrier) are well known concepts in precise positioning to eliminate common mode errors. Difference correlators extend this concept to the level of correlator values. By doing that, the same common mode errors are cancelled thereby drastically reducing the signal dynamics. Then longer filter times can be applied to reduce the noise and to eliminate multipath contributions. Difference correlators have been introduced in chapter 10 of [RD1], and will be recapitulated here. The algorithm of this paper goes beyond the one from the one of [RD1] by using longer coherent integration times and a batch filter.

Forming Differences

Forming differences at correlator level is a little tricky, as various ways to define the carrier phase are around and because the timing relationship of the data is important. In the following, the method of single difference forming and double difference forming are described and how undifferenced observations are then re-derived from them.

Single Differenc Correlator

Generally the classical receiver single difference carrier phase observation is defined via an equation like

$$\Delta\varphi^k\left(t^k\right)=\varphi^{k,rov}\left(t^k\right)-\varphi^{k,ref}\left(t^k\right)\cdot \qquad (1)$$

$\varphi^{k,rov}$ Rover carrier phase to satellite k [rad]

$\varphi^{k,ref}$ Reference carrier phase to satellite k [rad]

$\Delta\varphi^k$ Single difference carrier phase [rad]

The carrier phases are read from a RINEX file or a similar source (e.g. RTCM). The epoch t^k generally refers to the rover timescale, but if reference station observations are available at different epochs, then those timing errors can be tolerated if satellite positions are properly accounted for. This is usually done in many RTK software packages.

To form correlator differences, a slightly different approach is needed. First, the tracking channel outputs a carrier phase reading based on the internal NCO, which is not necessarily controlled by a PLL. Typically a FLL or vector tracking is used. In general, the internal tracking is not locked to the received carrier phase (due to bad signal conditions) and the difference between the received and internal carrier phase is contained in the prompt correlator. The received rover phase can be estimated by an expression like:

$$\exp\left\{i\varphi^{k,rov}\left(t\right)\right\}=\left|a\left(t\right)\right|\exp\left\{i\varphi^{k,NCO}\left(t\right)\right\}P^{k,rov}\left(t\right) \qquad (2)$$

$a(t)$ Amplitude function (not relevant here)

$\varphi^{k,NCO}$ Rover carrier phase to satellite k [rad] based on NCO reading while using internal FLL tracking

$P^{k,rov}$ Rover prompt correlator (complex valued) capturing the difference of the internal FLL tracking to the true received signal

Therefore a receiver single difference correlator is written as

$$\Delta P^k\left(t^k\right) = \\ = \exp\left\{i\varphi^{k,NCO}\left(t^k\right)\right\} P^{k,rov}\left(t^k\right)\exp\left\{-i\varphi^{k,ref}\left(t^k\right)\right\} d\left(t^k_{sent}\right) \cdot \quad (3)$$

d	Broadcast navigation data bit (if any)
ΔP	Single difference correlator

To wipe-off data bits we retrieve the broadcast data bit from the reference station corresponding to the sent time for the correlator value $P^{k,rov}$. We assume that the internal receiver time t^k is steered towards the true GPS time better than +/- 1 ms and the same applies for the reference receiver. Then we simply take t^k (which is a rover time) and use it as a reference station time to extract the reference station carrier phase. Later in (5) this process will be reversed, thereby compensating any timing error in the range. The satellite velocity and acceleration will be sufficiently accurate with this small timing error.

A filter (see next section) is applied to batches of single difference correlator values and the phase of the filtered correlator values is unwrapped:

$$\Delta Q^k\left(t\right) = F\left\{\Delta P^k\left(t\right)\right\} = \left|\Delta Q^k\left(t\right)\right|\exp\left\{i\Delta\eta^k\left(t\right)\right\} \quad (4)$$

ΔQ^k	Filtered single difference correlator
F	Batch filter
$\Delta\eta^k$	Unwrapped phase of the filtered single difference correlator [rad]

Finally the unwrapped phase is added to the reference station phase, thereby yielding the new improved undifferenced rover carrier phase, which is then written into the RINEX file or used otherwise:

$$\varphi^{k,rov}\left(t\right) = \Delta\eta^k\left(t\right) + \varphi^{k,ref}\left(t\right) \cdot \quad (5)$$

Reference Station Data Interpolation

The computation of (3) requires the evaluation of the reference station carrier phase at the rate of the correlator values (e.g. 50 Hz). The phase itself is typically available with a lower rate (e.g. 1 Hz). Therefore a suitable interpolation procedure has been designed. In a first step the nearest but earliest reference station epoch is located:

$$T^n = \arg\min_n\left(t_k - T^n\right)\Big|_{t_k > T^n} \quad (6)$$

T^n	Low rate (e.g. 1 Hz) reference data epochs
t^k	Correlator epochs (e.g. 50 Hz)

Then the carrier phase data at T^n, T^{n-1}, T^{n+1} are used to define a quadratic polynomial and to perform the interpolation. The interpolation scheme is designed in a way to give a continuous interpolation result; a change of the control point set only occurs when if $t^k = T^n$ and then both sets give identical results.

Double Difference Correlator

The double difference process forms satellite differences between two single difference correlators. The reference satellite gets the index l. It is typically the satellite with the highest elevation.

The double difference correlator is written as

$$\nabla\Delta P^{k,l}\left(t^k, t^l\right) = \Delta P^k\left(t^k\right)\overline{\Delta P^l\left(t^l\right)} \quad (7)$$

t^k	Other satellite epoch in [s] when a correlator value for the satellite k is available
$\nabla\Delta P$	Double difference correlator
l	Reference satellite index
k	Other satellite index

and depends on the two epochs of the two involved single difference correlators. Typically they are chosen to be the timely nearest correlator values. The later undifferencing process (9) or (10) will eliminate any errors introduced by asynchrony of the correlators for satellite k and l.

The adaptive filter is applied to the double difference correlator values and the resulting phase is unwrapped:

$$\nabla\Delta Q^{k,l}\left(t\right) = F\left\{\nabla\Delta P^{k,l}\left(t\right)\right\} = \left|\nabla\Delta Q^{k,l}\left(t\right)\right|\exp\left\{i\nabla\Delta\eta^{k,l}\left(t\right)\right\} \quad (8)$$

$\nabla\Delta Q$	Filtered double difference correlator
F	Batch filer
$\Delta\eta^{k,l}$	Unwrapped phase of the filtered double difference correlator [rad]

Undifferencing

Retrieving single difference (and finally undifferenced) observations from the double difference phase is not straight forward, because the receiver clock error has been completely eliminated during the double difference process. In the following two methods are proposed to re-introduce the receiver clock error.

Strongest Satellite Based Inversion

If a strong satellite is available (the reference satellite), its carrier phase might by estimated with the single difference approach or via undifferenced data. Then the single difference carrier phase of the other satellites is obtained by adding the double difference to the reference single difference. The undifferenced observations are finally obtained by the adding the carrier phases of the reference station:

$$\varphi^{k,rov}\left(t^k\right) = \nabla\Delta\eta^{k,l}\left(t^k, t^l\right) + \Delta\eta^l\left(t^l\right) + \varphi^{k,ref}\left(t^k\right) \quad (9)$$

Note, this calculation needs to be performed only for the RINEX output epoch.

Pseudorange Based Inversion

If single or undifferenced tracking can not be applied for the reference satellite, then we may chose to derive the carrier phase of the reference satellite from the code pseudorange. The undifferenced carrier phase of all satellites is given by

$$\varphi^{k,rov}\left(t^k\right) = \\ = \nabla\Delta\eta^{k,l}\left(t^k,t^l\right) + \frac{2\pi}{\lambda}R^{l,rov}\left(t^l\right) - \varphi^{l,ref}\left(t^l\right) + \varphi^{k,ref}\left(t^k\right) \quad (10)$$

$R^{l,rov}$ Code pseudorange of rover for reference satellite

λ Carrier wavelength [m]

Note, this calculation needs to be performed only for the RINEX output epoch.

Later, the RTK positioning will work with double difference observations. Any error introduced in the undifferenced carrier phase values due to the use of the code pseudorange via (10) will cancel. If the positioning algorithm works with undifferenced carrier phases, then errors introduced by (10) will affect the carrier phase based receiver clock estimate. The artificially introduced receiver clock error is quite high and directly relates to the code pseudorange accuracy of $R^{l,rov}$.

BLOCK DIAGRAM

The difference correlator scheme has been implemented using the API of the SX-NSR in a post-processing mode, like for e.g. [RD2]. In a first step rover signal samples are captured for L1 and L2 as well as reference station observations in RINEX3 format for L1 C/A and L2C plus the broadcast navigation data bits. In a second step all those data are processed and a RINEX file with the rover observations is obtained. Currently, the difference correlator scheme is applied only for carrier tracking. Rover code and Doppler observations are produced using standard tracking loops with (V)DLL or (V)FLL. The implemented difference correlator scheme is generally real-time capable, but momentarily reference station data is read in via a RINEX file. For real-time operation, e.g. RTCM could be used.

Figure 1 shows a block diagram of the difference correlator together with the key formulas of the preceding section.

The difference correlator mode works as a piggy bag module on-top the standard rover tracking. This can either been realized via DLL/FLL channels or via a vector tracking loop (VDLL/VFLL). The tracking channels output prompt I/Q correlator values for all tracked signals, which are buffered. Batches (synchronized to the RINEX observation rate) are formed. For each batch, the effect of the internal tracking is compensated. The reference station carrier phase is interpolated to the rover epoch, the data bit is retrieved from the assistance data base and the difference correlator is formed. The batches of difference correlator values are fed into the batch filter. This filter reduces multipath and noise. Using the filtered difference correlator values, the phase discriminator estimates the wrapped phase and the Doppler. The wrapped phase is compared to the wrapped phase estimate from the previous batch at the boundary epoch, thereby obtaining the unwrapped carrier phase. The difference of the two phase estimates should be near an integer value and is an indication, if a cycle-slip occurred. Finally, undifferencing is applied and the carrier phase is written together with the conventional code and Doppler observations into the RINEX file.

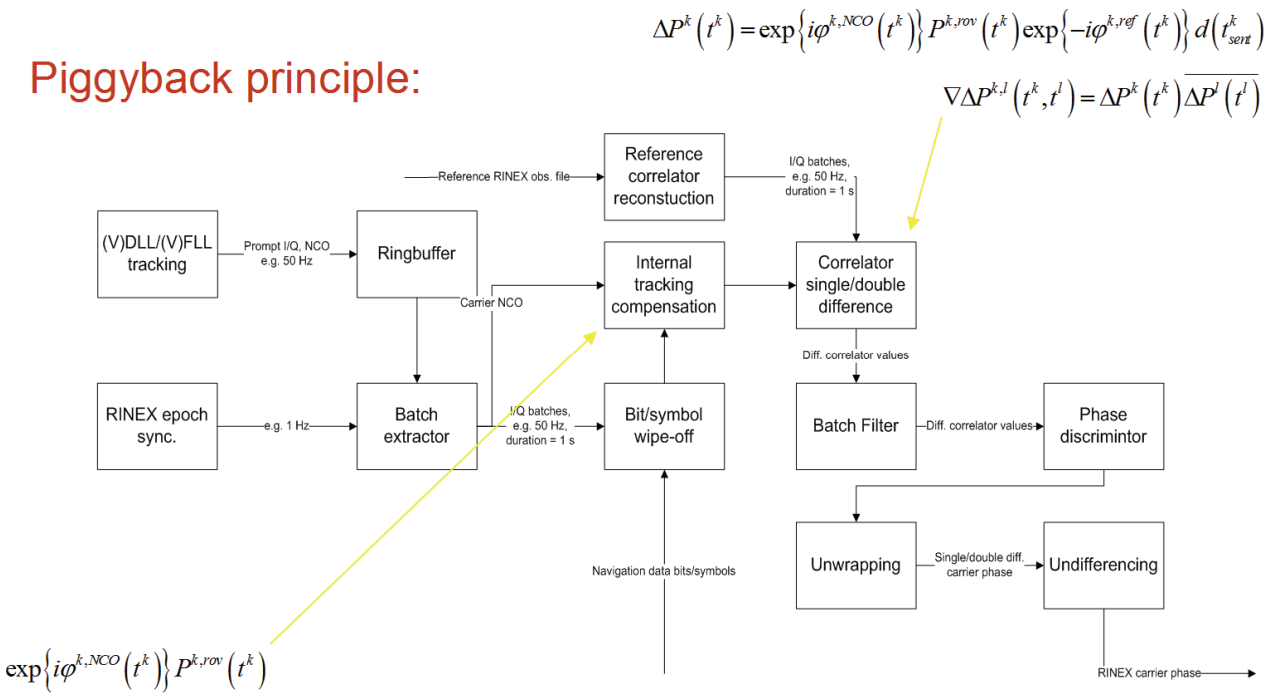

Figure 1. Block diagram of the difference correlator tracking scheme

BATCH PROCESSING

One innovative feature compared to the difference correlator approach of [RD1] is the use of correlator values batches to apply a dedicated filter and to use longer coherent integration times.

Correlator Batch Filters

The batch filter has been introduced in (4) and (8). Here, we will now give a detailed description.

Generally the adaptive filter F has the form

$$Q\left(t_\mu\right)=F\left\{P\left(t_\mu\right)\right\} \tag{11}$$

and converts raw correlator values P into filtered correlator values Q. The filter may work with undifferenced values, single or double differences. Two options will be described below: the cost minimization filter and the frequency domain filter.

Cost Minimization Filter

The cost minimization filter first fits a quadratic model to the batch of correlator values.

$$\hat{\varphi},\hat{f},\hat{a}=\arg\min_{\varphi,f,a}\sum_\mu\left(1-\cos\left(\arg\left\{P\left(t_\mu\right)\exp\left\{-i\left(2\pi ft_\mu+2\pi at_\mu^2+\varphi\right)\right\}\right\}\right)\right) \tag{12}$$

φ	Carrier phase offset [rad]
f	Doppler frequency [Hz]
a	Acceleration [Hz/s]

A 'hat' on a symbol denotes an estimated parameter. The admissible range for Doppler and acceleration values can be limited based on prior knowledge of the line-of-sight dynamics.

The estimation itself is carried out with a grid search algorithm for Doppler and acceleration. For fixed Doppler and acceleration values, the phase can be calculated analytically.

Based on the estimated parameters the filtered correlator values are given by

$$Q\left(t_\mu\right)=\exp\left\{i\left(2\pi\hat{f}t_\mu+2\pi\hat{a}t_\mu^2+\hat{\varphi}\right)\right\}\cdot \tag{13}$$

Frequency Domain Filter

The estimation in frequency domain first multiplies the correlator values by a proper windowing function h (e.g. a Hamming window)

$$P'(t_\mu) = P(t_\mu)\,h(t_\mu) \tag{14}$$

Then the vector length is increased to achieve a better frequency solution and the Fourier transform is computed.

$$\tilde{P}(f) = FFT\{P'\} \tag{15}$$

In the next step, the dominant spectral contribution is detected as:

$$\hat{f} = \arg\max_f \left|\tilde{P}(f)\right| \tag{16}$$

Spectral contributions which are beyond a certain threshold are assumed to be noise or multipath and are cancelled in frequency domain

$$F\{\tilde{P}(f)\} = \begin{cases} \tilde{P}(f) & \text{if} \quad \left|\tilde{P}(f)\right| \geq \gamma \left|\tilde{P}(\hat{f})\right| \\ 0 & \text{otherwise} \end{cases} \tag{17}$$

The threshold γ is typically 99 %.

Finally the filtered correlator values are obtained via an inverse Fourier transformation.

Sensitivity

Based on section 10.5.2 of [RD1] the noise variance of a difference correlator is expressed as

$$\mathrm{var}\langle\varphi\rangle = \frac{1}{2fT_{coh}C/N_0}\left(1+\frac{1}{2T_{coh}C/N_0}\right)+\frac{T_{coh}^2}{2f}\sigma_\omega^2 \cdot \tag{18}$$

φ	Carrier phase of a difference correlator [rad]
F	Factor (=1 for double difference, =2 for single difference)
T_{coh}	Coherent integration time [s]
σ_ω^2	Doppler accuracy [rad^2/s^2]

The phase noise is the sum of the discriminator noise and a term related to the interpolation of the phase values to the measurement epoch. The latter term is influenced by the Doppler tracking accuracy.

The thermal noise error is more or less identical for undifferenced and single difference operation as the noise contribution from the reference station data is very small due to the high received signal power.

For safe unwrapping a 6-sigma criterion can be applied, like

$$\mathrm{var}\langle\varphi\rangle < \left(\frac{\pi}{6}\right)^2 \cdot \tag{19}$$

The carrier phase noise is plotted as a function of C/N0 for different values of C/N0 and for two different coherent integration times in Figure 2. For the static case and an integration time of 100 s, extremely low C/N0 values seem to be possible. This is partly understood, because in that case we gather enough energy before computing the discriminator and the long integration time ensures high Doppler estimation accuracy. Of course, code and Doppler lock must be maintained, for example by vector tracking. Then at least four other signals with higher power may a force a channel to lock onto a very low power signal of e.g. -14 dBHz. The case of 200 ms is for more dynamic applications and compares approximately to the results of Figure 10.9 of [RD1] where a PLL tracking bandwidth of 1 Hz is used.

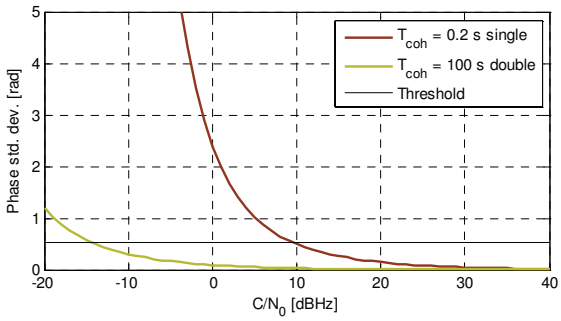

Figure 2. Carrier phase noise for single and double difference correlator

SIGNAL PROCESSING RESULTS

This section summarizes the results from two test campaigns.

Canopy Test

For the canopy test, the rover antenna (a Trimble Zephyr 2) was placed on the ground on a parking lot besides a small forest in Poing/Germany as shown in Figure 3. The tree branches covered the zenith direction of the antenna and free view was only to the North direction.

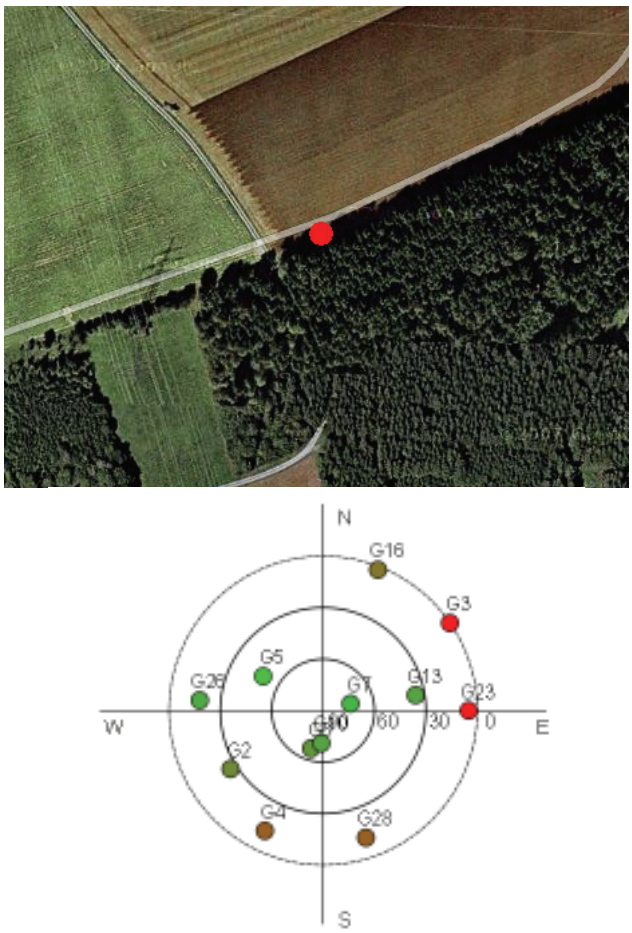

Figure 3. Measurement location and sky plot for the canopy test

The test was carried out during a period where 2 Block IIR-M satellites with the L2C signals were visible. As shown, they are PRN5 and 7. Signal samples for L1 and L2 were collected with the NavPort-4 frontend. The reference antenna was on the South roof of the IFEN office approximately 1.7 km away from test location.

Data Processing

The data has been analyzed in post-processing. In a first run, navigation data bits/symbols for L1C/A and L2CM have been extracted from the reference station data as well as a RINEX3 file. This data has then been fed into the double difference module to process the rover data with the settings of Table 1. The output of the processing is a RINEX file for the rover observations and for each integration interval, satellite and frequency, an intermediate log file has been produced containing correlator values and NCO values. These log files are analyzed in the following. As reference PRN we chose PRN5.

Parameter	Value
Code/Doppler tracking scheme	VDLL/VFLL (fixed position)
Carrier tracking scheme	Double
Integration time	5 s
Overlap	0.5 s
Carrier phase estimation	Cost function
Max./Min Doppler	+/- 5 Hz
Doppler grid points	801
Max./Min. acceleration	+/- 0 Hz/s
Acceleration grid points	-

Table 1. Canopy test processing parameter

Results

The estimated double difference carrier phase for PRN7 (reference PRN5) is shown in Figure 4. Prior to plotting a trend of 0.27 m/s was removed for better visualization. The curvature of the double difference carrier phase is mostly due to the satellite motion during the observation interval and due to atmospheric delay variations. The L1 and L2 result match well. During the plotting interval the phase difference increases from ~ 2 cm to ~ 5 cm. This can be attributed to ionospheric delay variations. The lines consist of small segments (each of 5 s duration). Each segment represents an uncorrelated double difference carrier phase estimate and a double difference Doppler estimate. The segments fit well to each other and phase differences at the boundaries are below 1-2 cm.

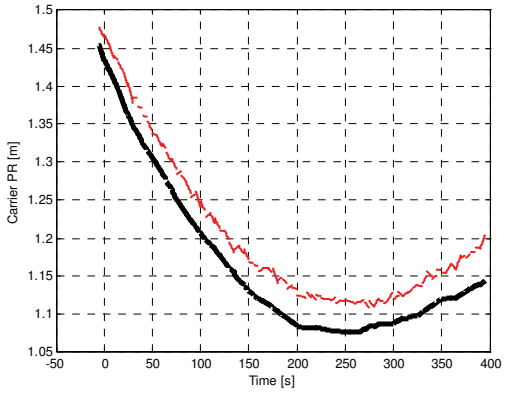

Figure 4. Double difference carrier phase for PRN7 (reference PRN 5) on L1C/A (black) and L2CM (red).

A similar plot is shown for PRN2 (reference PRN5) in Figure 5. PRN2 is a ~ 28° elevation satellite and received through the canopy. The double difference Doppler nearly vanishes and no trend has been subtracted prior to plotting. During t = 90 – 170 s the double difference carrier phase shows a higher dynamics. This is probably due to refraction effects (trunks,…) but might also be caused by the ionosphere. The individual batches suggest that the overall phase is estimated smoothly and no cycle-slips occurred.

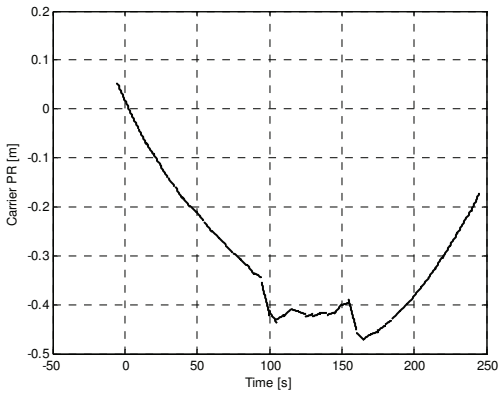

Figure 5. Double difference carrier phase for PRN2 (reference PRN 5) on L1C/A

Data for the low elevation ~ 10° satellite PRN28 (reference PRN5) is shown in Figure 6. The PRN28 signal has to pass a large forest area (maybe 50-100 m) before it reaches the rover antenna. The plot shows a smooth behavior and the single batches suggest that even this degraded signal is tracked without cycle slips. The zoom of PRN28 shows that carrier phase gaps between the single batches are below 0.5 cm.

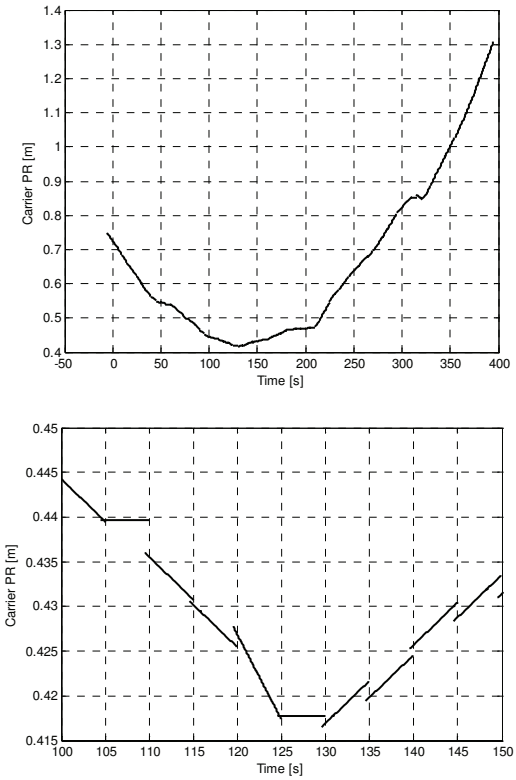

Figure 6. Double difference carrier phase for PRN28 (reference PRN 5) on L1C/A (lower figures is a zoom of the upper figure)

Interpretation

The canopy test shows promising results from the signal processing point of view. Even low elevation satellites are tracked without any cycle slips and the L1/L2 comparison gives consistent results. Further tests with more L2C signals would be helpful to consolidate the results.

Indoor Test

During the difference correlator experiments, the need for precisely surveyed indoor reference points became obvious. Only with their help, it would be possible to judge the precision of the carrier phase measurements. Therefore, IFEN requested from a surveying office to measure the coordinates of indoor points together with the coordinates of the two roof antennas. All coordinates have a precision of around 0.5 cm.

For the indoor L1/L2 experiment, we placed the antenna phase center of a Trimble Zephyr 2 antenna 1.651 m above the point 133 inside the office and used as reference antenna IFEN2. Approximately two hours of data have been collected at a period where 4 L2C capable satellites (12, 25, 29, 31) were visible. The office has a window to the North of point 133. The elevation angle of the upper window border is around 25° (i.e. all satellites having an elevation higher than 25° have to penetrate at least one wall before reception by the indoor antenna). A skyplot is shown in Figure 7.

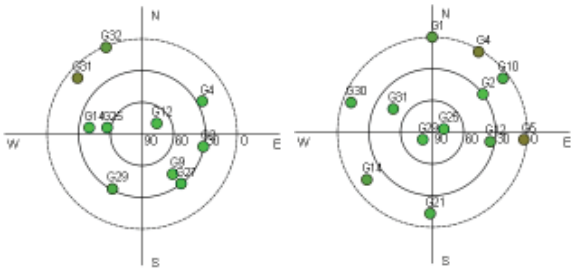

Figure 7. Skyplot at the beginning (left) and end (right) of the L1/L2 indoor experiment

Data Processing

The data processing has been done in the usual way in post-processing. The processing parameters are summarized in Table 2.

Parameter	Value
Code/Doppler tracking scheme	VDLL/VFLL (fixed position)
Carrier tracking scheme	Double
Integration time	30 s
Overlap	0.2 s
Carrier phase estimation	Cost function
Max./Min Doppler	+/- 0.05 Hz
Doppler grid points	81
Max./Min. acceleration	+/- 0.0001 Hz/s
Acceleration grid points	41

Table 2. Indoor processing parameter

Results

A typical good result of the carrier tracking performance is PRN25 with PRN12 being used as reference satellite. Both signals penetrate the ceiling to reach the indoor antenna. The L1 and L2 carrier phase estimates are to high degree consistent and reflect the geometric motion of the satellite as can be seen from Figure 8. Also Doppler (slope) and phase estimates are consistent and the signal processing does not detect any cycle slips. The only difficult period is at t ~ 3450 – 3600 s on L2CM. During this time fading on L2 occurs; cf. lower part of Figure 8. However, the spectrum of the double difference correlator shows still a clearly visible peak and we argue that the estimates are not corrupted by excessive noise; cf. Figure 10. However, the L2 estimates experience a cycle slip as shown in Figure 9. The cycle slip develops over a period of around 100 seconds and during this period Doppler and phase estimates are slightly less consistent than during normal tracking. The 30 s batches still show phase gaps of less than 2 cm and the signal processing does not detect them as cycle-slips.

Another good satellite combination is PRN29 (reference PRN12) and the results are shown in Figure 11. Again both satellite signals are received through the ceiling.

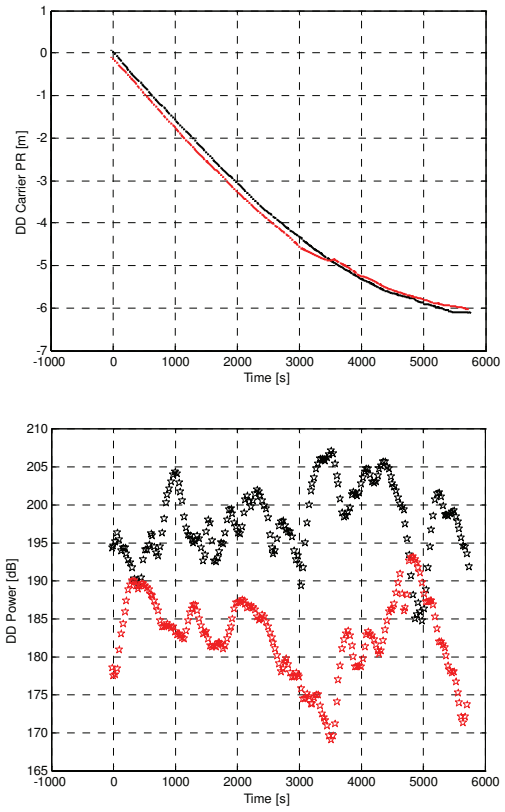

Figure 8. Double difference carrier phase and signal amplitude for PRN25 (reference PRN 12) on L1C/A (black) and L2CM (red).

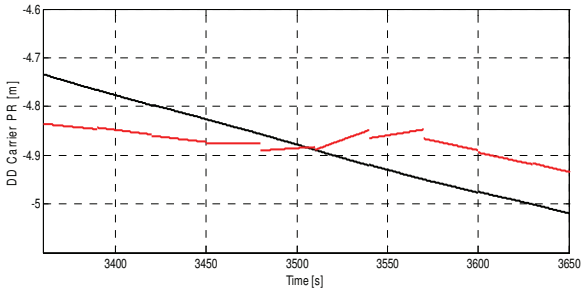

Figure 9. Zoom into Figure 8.

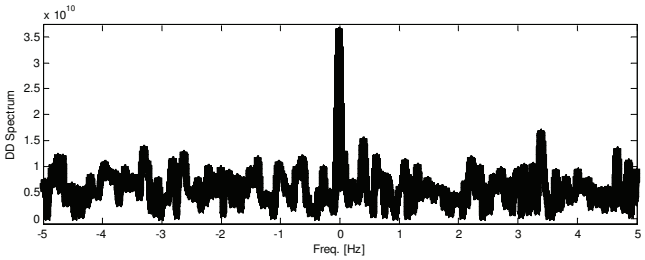

Figure 10. L2CM double-difference correlator spectrum (black) at t = 3540-3570 of Figure 8.

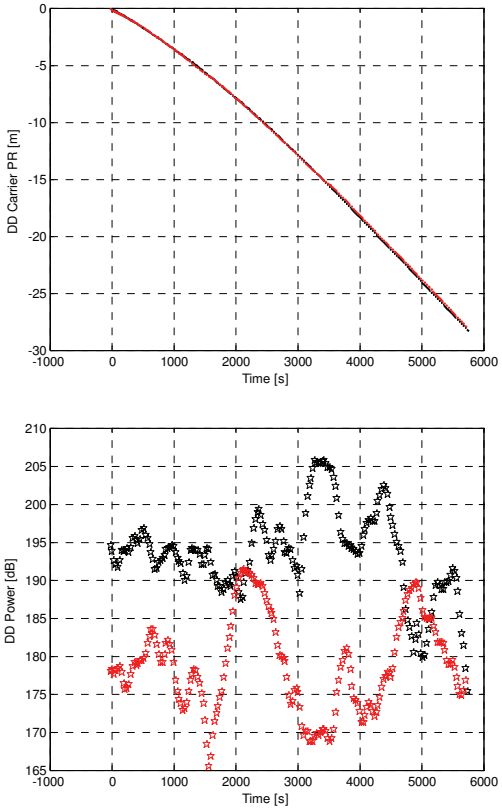

Figure 11. Double difference carrier phase and signal amplitude for PRN29 (reference PRN 12) on L1C/A (black) and L2CM (red).

Using the known coordinates, we are able to subtract the geometric distance from the double difference carrier phase observations and plot the results for the wide-line linear combination. However, in reality we do not know the ground-truth and, therefore, we need a different measure for identification of suitable observation sections. Double differences of phase ranges (carrier phase observation converted to meters) of both frequencies shall show similar patterns. Since the distance to the reference station is very short, only a couple of 10 meters, the ionospheric effects are completely removed in our case. The difference of L2 phase range double differences minus L1 phase range double differences are shown in Figure 12. For plotting, these metric values have been converted back to L2 cycles. PRN25 has been chosen as the reference satellite for building the double differences. The curves of PRN12 and PRN29 are rather flat indicating a rather good agreement of L1 and L2 phase observations. The values for PRN31 are showing larger excursions. However, the signal processing for PRN31 indicated severe tracking problems, which are showing up here.

Overall, one can identify rather good sections of 10 minutes from 346300 to 346900 and of about 16 minutes at the end (347310 to 348270).

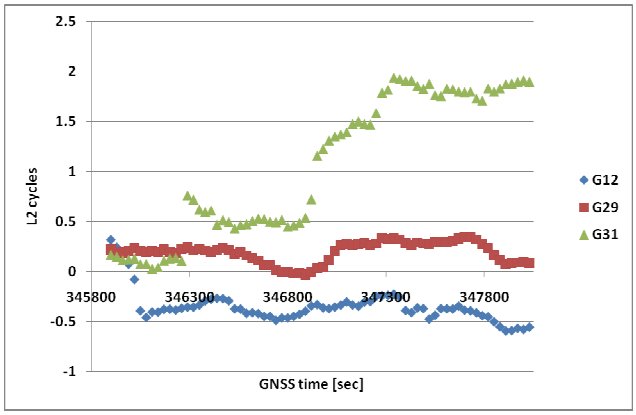

Figure 12. L2 double difference phase ranges minus L1 double difference phase ranges converted to L2 cycles

Interpretation

This static L1/L2 indoor test verifies the ability of the method to track the carrier phase of indoor signals. The method, however, also potentially may track reflected signals very stably. A consistency analysis of L1 and L2 data might be used as a decision criterion to check the validity of the data. With the known geometry, we can investigate biases on the double-difference carrier phases. Strong biases seem to be present and they could be well explained by refractivity variations of the penetrated building materials. For example [RD3] predicts a propagation speed of 61 % of the speed of light for lumber, of 49 % for bricks and 43 for % concrete. Thus, delays on the order of the wavelength are easily possible. Furthermore, reflections at the wall boundaries complicate the problem.

USE IN POSITIONING

The carrier phases obtained in the indoor scenario do not have blunt jumps suggesting the occurrence of cycle slips. Therefore, these carrier phases may provide a reasonable positioning quality. Knowing that the pseudorange quality is not sufficient, we decided to base the positioning mainly on the carrier phases. The pseudoranges have to be down-weighted drastically so that the baseline computation is effectively identical to a phase only differential positioning. It is well-known that phase only computations rely heavily on satellite geometry changes for determination of positioning. Under open sky scenarios this has been the traditional method of precise differential positioning a couple of decades back. The open question was for us, does the indoor observation still have enough signal of the satellite geometry itself or is the whole dataset contaminated by multipath reflections to prevent any reasonable positioning result?

The carrier phase observations have been processed using inPosition's processing software. We have used all carrier phase observations available. The carrier phases on L2 were only available for PRN12, PRN25, PRN29 and PRN31. These satellites allowed tracking L2C code. However, more satellites allowed L1 carrier phase

tracking. The complete carrier phase information of satellites above an elevation mask of 15 degrees have been used in our baseline computations.

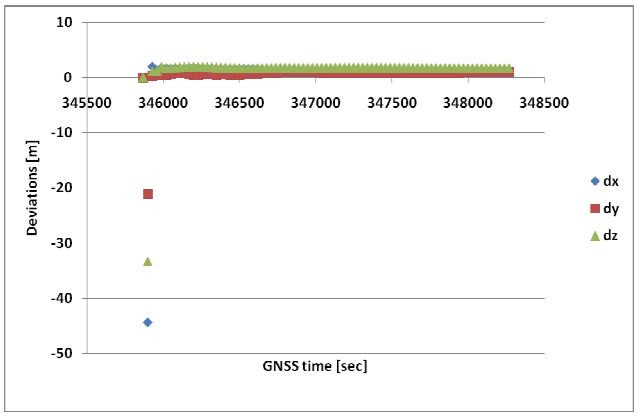

Figure 13. Coordinate convergence for floating ambiguity computation; time interval 345870 to 348270.

Figure 13 shows the true convergence errors of the floating ambiguity computation of the whole time interval analyzed. Since the computation is mainly dependent on the carrier phases the initial positions are far off, but the convergence settles the results very fast. Figure 14 shows the same results zoomed to high-light the epoch to epoch stability of the positioning. The overall deviation of the results does not improve significantly over the complete observation interval. Besides the dx component the deviations have settled already within the first 10 minutes.

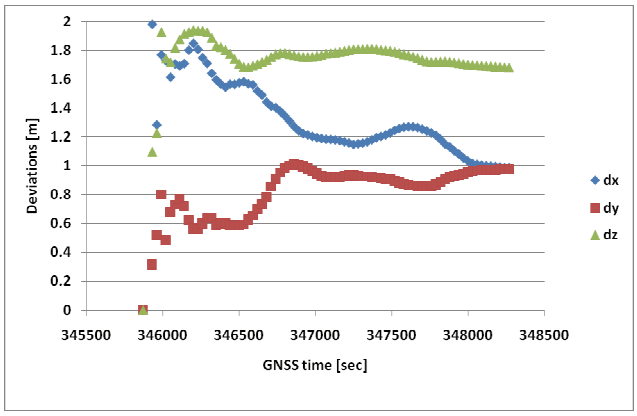

Figure 14. Coordinate convergence for floating ambiguity computation; time interval 345870 to 348270 (first epochs removed).

As already recognized earlier the carrier phase tracking of some satellites have had some difficulties during the in-door test. As discussed for Figure 12 the carrier for PRN31 showed some unfavorable drift in the mid of the interval. We computed the baseline with carrier phase observations limited to the two favorable sections indicated through visual inspection of the differences of double differenced L1 and L2 phase ranges.

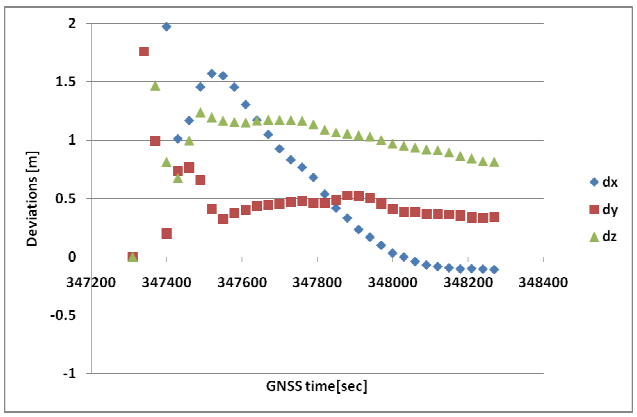

Figure 15. Coordinate convergence for floating ambiguity computation; time interval 347310 to 348270 (first epochs removed).

The positioning results based on the last 16 minutes of the whole observation interval are given in Figure 15. The results of the first epochs have been clipped because they are outside of the plot range. Those values have been around 10-15 meter deviations as to be expected from our earlier computations.

Table 3 shows the summary of deviations at the end of each computation interval in horizontal and vertical components. Especially the computation of the last observation section of 16 minutes shows that the overall length of the whole computation interval is the major contribution for convergence. For the data analyzed the convergence settled quite fast. Since the carrier phase inhibit some biases due to the penetration of the different materials the integer ambiguity resolution was invoked. Further investigations especially on the indoor is required.

Start	Stop	dN [m]	dE [m]	dUp [m]	Len [m]
345870	348270	-0.252	-0.752	-2.032	2.182
347310	348270	-0.566	-0.357	-0.584	0.888
346290	346890	-0.231	-1.034	-2.077	2.331

Table 3. Summary of indoor positioning runs

CONCLUSIONS

Difference correlators represent an effective mean to remove signal dynamics from correlator values and to increase the coherent integration time drastically. The concept can be implemented as piggyback module to conventional DLL/FLL tracking. Depending on the use case, satellite or receiver single difference correlator might be used or double difference correlators. For static differential positioning, the use of double difference correlators seems to be the method of choice allowing coherent integrations times of several hundreds of seconds.

Despite the fact that some of the carrier phase observations have been collected indoor these observations are not pure sampled arbitrary reflections of

the original signals. The carrier phase observations are continuous and allow the application of sophisticated differential carrier processing. The deviations to the truth of around 2 m respectively less than 1 meter are exceptional good for the environment chosen. Our analysis has just started and has to continue.

ACKNOWLEDGEMENTS

The research has received funding from the European Community's Seventh Framework Programme (FP7/2007-2013) under grant agreement n° 247866.

REFERENCES

[RD1] Navigation Signal Processing for GNSS Software Receivers Pany, T.: Artech House, 2010, ISBN: 978-1-60807-027-5 - 2010

[RD2] Coherent Integration Time: The Longer, the Better Pany et al., InsideGNSS, vol. 4, no. 6 – 2009

[RD3] GNSS Indoors: Fighting the Fading, Part 2 Hein et al.: InsideGNSS May/June 2008